

Article

Thermal Efficiency and Economics of a Boil-Off Hydrogen Re-Liquefaction System Considering the Energy Efficiency Design Index for Liquid Hydrogen Carriers

Minsoo Choi ¹, Wongwan Jung ¹, Sanghyuk Lee ², Taehwan Joung ³ and Daejun Chang ^{1,*}

¹ Department of Mechanical Engineering, Korea Advanced Institute of Science and Technology (KAIST), Daejeon 34141, Korea; minsoo.choi@kaist.ac.kr (M.C.); wjung@kaist.ac.kr (W.J.)

² Energy Plant Research Center, Samsung Heavy Industries, Seongnam-si 13486, Korea; sh.91.lee@samsung.com

³ International Maritime Research Center (IMRC), Korea Research Institute of Ships & Ocean Engineering (KRISO), Daejeon 34103, Korea; thjung@kriso.re.kr

* Correspondence: djchang@kaist.ac.kr; Tel.: +82-42-350-1514

Abstract: This study analyzes the thermodynamic, economic, and regulatory aspects of boil-off hydrogen (BOH) in liquid hydrogen (LH₂) carriers that can be re-liquefied using a proposed re-liquefaction system or used as fuel in a fuel cell stack. Five LH₂ carriers sailing between two designated ports are considered in a case study. The specific energy consumption of the proposed re-liquefaction system varies from 8.22 to 10.80 kWh/kg as the re-liquefaction-to-generation fraction (R/G fraction) is varied. The economic evaluation results show that the cost of re-liquefaction decreases as the re-liquefied flow rate increases and converges to 1.5 \$/kg at an adequately large flow rate. Three energy efficient design index (EEDI) candidates are proposed to determine feasible R/G fractions: an EEDI equivalent to that of LNG carriers, an EEDI that considers the energy density of LH₂, and no EEDI restrictions. The first EEDI candidate is so strict that the majority of the BOH should be used as fuel. In the case of the second EEDI candidate, the permissible R/G fraction is between 25% and 33%. If the EEDI is not applied for LH₂ carriers, as in the third candidate, the specific life-cycle cost decreases to 67% compared with the first EEDI regulation.

Keywords: liquid hydrogen carrier; boil-off hydrogen; specific energy consumption; exergy efficiency; economics; energy efficiency design index



Citation: Choi, M.; Jung, W.; Lee, S.; Joung, T.; Chang, D. Thermal Efficiency and Economics of a Boil-Off Hydrogen Re-Liquefaction System Considering the Energy Efficiency Design Index for Liquid Hydrogen Carriers. *Energies* **2021**, *14*, 4566. <https://doi.org/10.3390/en14154566>

Academic Editor: Bahman Shabani

Received: 21 June 2021

Accepted: 20 July 2021

Published: 28 July 2021

Publisher's Note: MDPI stays neutral with regard to jurisdictional claims in published maps and institutional affiliations.



Copyright: © 2021 by the authors. Licensee MDPI, Basel, Switzerland. This article is an open access article distributed under the terms and conditions of the Creative Commons Attribution (CC BY) license (<https://creativecommons.org/licenses/by/4.0/>).

1. Introduction

Due to the current global attention concerning the reduction of carbon dioxide (CO₂) emissions, which is the largest contributor to global warming [1], the demand for renewable energy is increasing. A large portion of CO₂ emissions is attributed to the combustion of the fossil fuels, which provide approximately 80% of the total world energy supply [2]. From 2009 to 2018, global CO₂ emissions increased by 16% [3]. To reduce CO₂ emissions, power generation using renewable energy, which is not accompanied by CO₂ emissions, has been increasing. According to the International Energy Agency, power generation achieved using renewable energy has increased by 57% from 2010 to 2018 [4]. The portion of renewable energy used for electricity generation has been projected to consistently increase in the future [5].

Although renewable energy can be used to reduce CO₂ emissions, its production varies from region to region. This uneven distribution of renewable energy requires the use of energy carriers that can transport surplus renewable energy. Hydrogen is regarded as a potential energy carrier candidate for storing and transporting surplus renewable energy over long distances [6]. The delivered hydrogen generates energy from an oxidation process in fuel cells, which produces no CO₂ and only pure water [7]. Hydrogen also has other principal advantages as an energy carrier, as noted by Rosen et al. [8]. It is

free from exhaustion because it can be obtained by electrolyzing water into oxygen and hydrogen. Additionally, unlike electricity itself, it can be stored in a variety of forms such as compressed gas, liquid, and in chemical compounds including ammonia and metal hydrides [9].

Considering the large-scale transportation of hydrogen, it is essential to develop liquid hydrogen (LH₂) carriers. LH₂ has a density of 70 kg/m³, which is higher than the density of compressed hydrogen (39 kg/m³) at 70 MPa [10]. Compared to ammonia, LH₂ is safer, as it is nontoxic. Moreover, because it is a pure substance that is not combined with other elements, it does not require any additional energy or processes to break its chemical bonds.

The main challenge concerning the transportation of hydrogen in a liquid state is its cryogenic boiling temperature, which is 20 K at atmospheric pressure. Although LH₂ storage tanks on land are heavily equipped with an insulation layer, heat ingress is inevitable [11], resulting in the generation of boil-off hydrogen (BOH) and increase in the pressure of the storage tank if no preventative measures are used. This issue also exists for LH₂ cargo tanks used in LH₂ carriers.

In the case of relatively large-scale liquefied natural gas (LNG) carriers, whose cargo temperature is around 110 K, a boil-off gas (BOG) re-liquefaction system is usually installed. This system extracts the BOG from the cargo tanks, re-liquefies it using a refrigeration cycle, and returns the re-liquefied BOG to the cargo tank. Many studies have been conducted concerning this BOG re-liquefaction system [12–15]. Romero et al. analyzed and evaluated the conditions, parameters, and energy consumption of a reverse Brayton cycle-based BOG re-liquefaction system [16]. Kwak et al. investigated a small-scale BOG re-liquefaction system for use on LNG-fueled ships. They optimized the nitrogen reverse Brayton cycle using a genetic algorithm and compared two cases with and without BOG compressors [17]. Yin et al. compared a reverse Brayton cycle-based BOG re-liquefaction system with two expanders to such a system with a single expander. They simulated two cycles using parallel and serial nitrogen expanders and compared them with the base case that possessed a single expander [18]. Sayyaadi et al. used a genetic algorithm to optimize the price of the BOG re-liquefaction system products [19]. In these previous studies of BOG re-liquefaction systems, the specific energy consumption (SEC), which indicates the energy required to re-liquify 1 kg of BOG, was found to be between 0.73 to 1.41 kWh/kg. This value varied depending on the inlet conditions of the BOG system. Moreover, the precooling and precompression processes affected the SEC. The reverse helium Brayton cycle for BOG re-liquefaction was preferred because it was easy to operate. Additionally, this cycle did not require high pressures and was more appropriate for onboard systems in terms of safety [17]. These studies can be utilized to design appropriate BOH re-liquefaction systems.

Many studies have been conducted to liquefy hydrogen from ambient temperatures [20–22]. The main results of these investigations may also be applied towards designing BOH re-liquefaction systems. Chang et al. analyzed and compared various figures of hydrogen liquefaction systems in terms of exergy efficiency [23]. In their study, the reverse Brayton cycle with two expanders showed an exergy efficiency of 24.2%, while the Claude cycle had an exergy efficiency of 27.2%. Asadnia et al. proposed a hydrogen liquefaction system using combined mixed refrigerants [24]. They separated the cycles into two sections, in which the first section was used for precooling and the second was used for cryogenic liquefaction. In the precooling section, 11 materials including hydrocarbons were used as a mixed refrigerant. In the cryogenic section, hydrogen, helium and neon were used as mixed refrigerants. The simulation results showed an SEC of 7.69 kWh/kg. Sadaghiani et al. also proposed a hydrogen liquefaction system that used mixed refrigerants [25]. The proposed system was composed of two cycles, one of which used a mixture of hydrocarbons while the other used a mixture of hydrogen, neon and helium as a mixed refrigerant. This system demonstrated an SEC of 4.41 kWh/kg. Chang et al. proposed a hydrogen liquefaction system that utilized the cold energy of LNG [26]. In that study, the LNG pre-cooled the hydrogen and was vaporized after precooling. Following the design of a hydrogen liquefaction system using LNG precooling, three configurations of the liquefac-

tion cycles were compared in terms of their energy consumption. Considering the required energy for the liquefaction process described in their paper, the SEC for the most efficient configuration was calculated as 17.37 kWh/kg, which includes the energy consumed for ortho-para conversion. Yuksel et al. also proposed a hydrogen liquefaction system with four serial helium turbo expanders and analyzed this system [27]. These previous studies showed that the SECs of hydrogen liquefaction systems vary with the configuration of the system and the inlet conditions of the hydrogen.

BOH re-liquefaction systems, however, differ from liquefaction systems for hydrogen at ambient temperatures. The temperature of BOH is much lower than the ambient temperature. Additionally, such a system does not require an ortho-para conversion process because the LH₂ in the cargo tank has already been converted into para-hydrogen. Lee et al. proposed a partial BOH re-liquefaction system for use on an LH₂ carrier [28]. In their study, some of the BOH from the LH₂ cargo tank was used as a fuel in a proton-exchange membrane fuel cell (PEMFC). The remainder was precompressed to 40 bar using a cold compressor with an inlet temperature of 120 K. This compressed BOH was cooled down using helium in a reverse Brayton cycle and re-liquefied by expansion. This BOH re-liquefaction system exhibited an SEC of 3.30 kWh/kg and exergy efficiency of 74.9%.

Previous studies of BOH re-liquefaction systems lacked an investigation of the economic feasibility of these systems that considered the installation and operation costs. A comparison with the production costs of LH₂ can be used to investigate the economic feasibility of BOH re-liquefaction systems. Moreover, considering that existing LNG carriers vary in terms of their capacity, economic case studies of BOH re-liquefaction systems with varying capacities are required.

Another critical factor to consider in the design and operation of the BOH re-liquefaction system is the energy efficiency design index (EEDI) regulation of LH₂ carriers. The EEDI is the design indicator regulated by the International Maritime Organization (IMO), which restricts the CO₂ emissions of ships during the design process. Ship of certain types as indicated by the IMO must obey this index to operate. The EEDI also affects the electricity generation of BOH re-liquefaction systems. However, such a regulation for LH₂ carriers has not yet been established. LH₂ is similar to conventional liquefied gases such as LNG and liquefied petroleum gas (LPG) in that it is liquefied. However, liquid hydrogen differs from other conventional liquefied gases because it is an extremely low-density liquefied gas that is free from CO₂ emissions. Consequently, the establishment of EEDI regulations for LH₂ carriers is difficult in comparison with that of other liquefied gases.

The objective of this study is to investigate the thermodynamic, economic, and regulatory aspects of BOH in LH₂ carriers in which the BOH can be either re-liquefied using the proposed re-liquefaction system or used as fuel for the fuel cells. A case study is conducted that considers five LH₂ carriers sailing between two designated ports. A thermodynamic analysis is carried out, followed by an economic assessment considering the re-liquefaction-to-generation (R/G) fraction. As these evaluations are meaningful in terms of the allowable EEDI, three EEDI candidates are proposed for estimating a feasible R/G fraction.

2. Proposed Boil-Off Hydrogen Re-Liquefaction System Combined with Fuel Cells

Figure 1 shows a process flow diagram of the proposed system. The system consists of a re-liquefaction cycle and PEMFC stack. The proposed re-liquefaction cycle is modified from a reverse Brayton cycle to utilize the cold energy of BOH heading to the PEMFC stack. The BOH to be utilized in the PEMFC stacks is first heated to the operating temperature of the PEMFC system. HX 1 and HX 3 are introduced to transfer the cold energy of the BOH to the helium refrigerant and increase the BOH temperature to the ambient temperature. Stream 101 indicates the BOH generation from the cargo tank. This stream is divided into two streams, which are labelled as 102 and 106. Stream 102 is cooled down and re-liquefied to a subcooled liquid state. Stream 106 cools the helium refrigerant and is utilized for propulsion. Stream 201 indicates the low-pressure helium stream. This stream is pressurized to a high pressure through Comp 1 and Comp 2. After AC 1, the helium

is cooled down along with the BOH heading to the PEMFC system. After the helium is compressed, it is cooled down using the cold helium in HX 4. It is then primarily expanded to an intermediate pressure via EXP 1 and cooled down via HX 5. After passing through HX 5, the helium is expanded to a low pressure through EXP 2 and the BOH is liquefied in HX 6. After the BOH has been re-liquefied, this cold helium then cools down the hot helium and hydrogen.

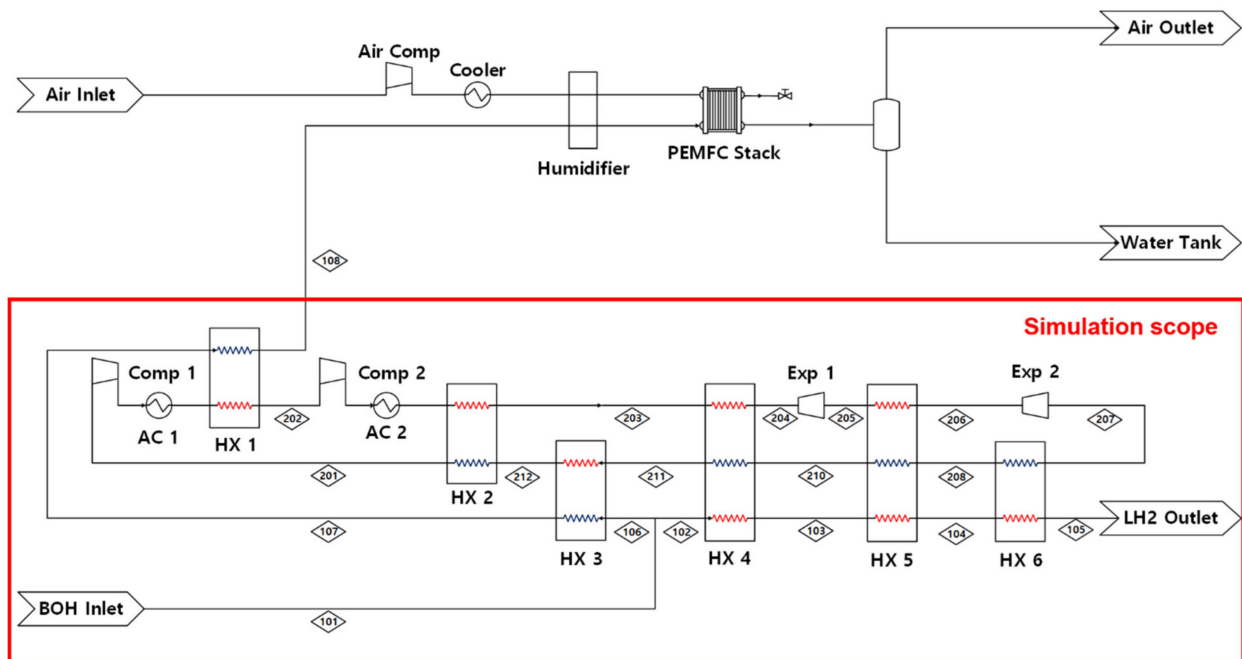


Figure 1. Process flow diagram of the proposed system.

Aspen Hysys V11 was used to simulate the proposed system. The modified Benedict-Webb-Rubin equation was applied for the states of ortho- and para-hydrogen. The Aspen properties (RefProp) were used for helium. Table 1 shows the boundary conditions for the process simulation.

Table 1. Boundary conditions of the BOH re-liquefaction cycle.

Item	Unit	Value
Cargo LH ₂ density	kg/m ³	70.83
Boil off rate	%/day	0.2 [29]
BOH inlet temperature	K	80
BOH outlet temperature	K	20
BOH pressure	bar	1.013

The following assumptions were made for this simulation:

- The dead-state temperature and pressure are 298 K and 1.01 bar, respectively.
- The temperature at the exit of the aftercooler is 313 K.
- The minimum temperature at the inlet of the compressor is 240 K.
- The high and low pressures of the helium cycle are 10 and 1.2 bar, respectively.
- The adiabatic efficiencies of the compressors are 75%.
- The adiabatic efficiencies of the expanders are 75%.
- The pressure drop in the heat exchangers is negligible.
- In the heat exchangers, the minimum temperature difference is larger than 1% of the hottest stream temperature. If the temperature of the hottest stream in the heat exchanger is greater than 300 K, the minimum temperature difference is 3 K [23,26].

3. Method of Evaluation

3.1. Energy and Exergy Efficiency

The total energy required to re-liquefy BOH is calculated using Equation (1).

$$\dot{W}_{\text{net}} = \dot{W}_{\text{Comp 1}} + \dot{W}_{\text{Comp 2}} - \dot{W}_{\text{Exp 1}} - \dot{W}_{\text{Exp 2}} \quad (1)$$

\dot{W}_{net} : Total work required to re-liquefy BOH

$\dot{W}_{\text{Comp 1}}$: Work input for Comp 1

$\dot{W}_{\text{Comp 2}}$: Work input for Comp 2

$\dot{W}_{\text{Exp 1}}$: Work output for Exp 1

$\dot{W}_{\text{Exp 2}}$: Work output for Exp 2

The R/G fraction, which is the ratio of the re-liquefied flow rate to the BOH generation flow rate, is estimated using Equation (2). The SEC is defined by Equation (3) to evaluate the energy required to re-liquefy the 1 kg of BOH. Because the re-liquefaction system utilizes the cold energy of the hydrogen, the SEC varies with the R/G fraction.

$$\text{R/G fraction} = \frac{\dot{m}_{\text{re-liquefaction}}}{\dot{m}_{\text{BOH-generation}}} \times 100 \% \quad (2)$$

$$\text{SEC} = \frac{\dot{W}_{\text{net}}}{\dot{m}_{\text{re-liquefaction}}} \quad (3)$$

$\dot{m}_{\text{BOH-generation}}$: Mass flow rate of the generated BOH

$\dot{m}_{\text{re-liquefaction}}$: Mass flow rate of the re-liquefied BOH

In thermodynamics, physical flow exergy refers to the maximum useful work delivered to an external user as the stream reaches the dead state [30]. Considering refrigeration systems, it refers to the reversible and minimum work required for refrigeration to occur at a certain state. The physical flow exergy of stream can be estimated using Equation (4) [31]. In Equation (4), subscripts S and 0 refer to present state of the stream and dead state, respectively. Subscript ** means state that has same temperature with the dead state and same pressure with the present state. The first two terms in Equation (4) corresponds to thermal exergy, which is the physical exergy from the temperature difference of the stream with the dead state. The last two terms represent mechanical exergy, which is the physical exergy from pressure difference of the stream with the dead state.

$$E_S = E_T + E_M = (H_S - H_{**}) - T_0(S_S - S_{**}) + T_0(S_0 - S_{**}) - (H_0 - H_{**}) \quad (4)$$

E_S : Physical flow exergy of stream

E_T : Thermal exergy of stream

E_M : Mechanical exergy of stream

H_S : Enthalpy of stream at present state

H_{**} : Enthalpy of stream at state **

H_0 : Enthalpy of stream at dead state

S_S : Entropy of stream at present state

S_{**} : Entropy of stream at state **

S_0 : Entropy of stream at dead state

T_0 : Ambient temperature

During re-liquefaction, the irreversibility between processes causes exergy loss. To calculate this exergy loss, the physical exergy difference between inlets and outlets of a component can be used [32]. This exergy loss makes the system less efficient and require

more work than an ideal system. From this point of view, the system exergy efficiency can be estimated using the numerical indicator η_{ex} via Equation (5).

$$\eta_{ex} = \frac{\dot{E}_{re-liquefaction-in} - \dot{E}_{re-liquefaction-outlet}}{\dot{W}_{net} + \dot{E}_{BOH\ to\ PEMFC-in} - \dot{E}_{BOH\ to\ PEMFC-out}} \quad (5)$$

$\dot{E}_{re-liquefaction-in}$: Physical flow exergy of Stream 102

$\dot{E}_{re-liquefaction-outlet}$: Physical flow exergy of Stream 105

$\dot{E}_{BOH\ to\ PEMFC-in}$: Physical flow exergy of Stream 106

$\dot{E}_{BOH\ to\ PEMFC-out}$: Physical flow exergy of Stream 108

3.2. Economics

CAPEX is defined as the initial investment required to construct a plant [33], and it consists of the direct project expenses, indirect project expenses, contingency and fee as depicted in Figure 2. The direct expenses encompass the equipment costs, material costs, and labor costs required to install the equipment. The indirect project expenses include the freight costs, insurance, and taxes. They also include the overhead costs required to construct the plant. The contingency is the cost that covers unforeseen circumstances, while the fee is related to the contractors. Among these costs, the sum of the direct and indirect costs is called the bare module cost. The contingency and fee are assumed as 15% and 3% of the bare module cost, respectively. The bare module cost for each component is estimated using the Aspen Capital Cost Estimator V11.

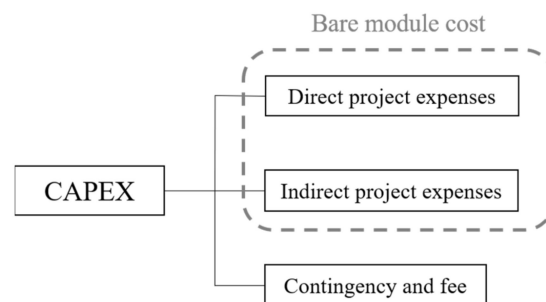


Figure 2. Composition of CAPEX.

OPEX is defined as the costs associated with the day-to-day operations of a plant [33]. OPEX consists of direct manufacturing costs, fixed manufacturing costs, and general manufacturing expenses as depicted in Figure 3. The direct manufacturing costs are the operating expenses, which vary with the production rate. They include raw materials costs, utilities costs, and operational labor. The fixed costs are independent of changes in the production rate. They include taxes and insurance. The general expenses are overhead costs that are necessary to carry out business functions. They include administration, distribution and selling costs, as well as costs for research and development. Equation (6) [33] is used to estimate OPEX. Table 2 shows the specific values used to estimate CAPEX and OPEX.

$$OPEX = 0.18 CAPEX + 2.73 C_{OL} + 1.23 (C_{UT} + C_{WT}) \quad (6)$$

C_{OL} : Cost of the operator salary

C_{UT} : Cost of utilities

C_{WT} : Cost of the cooling water

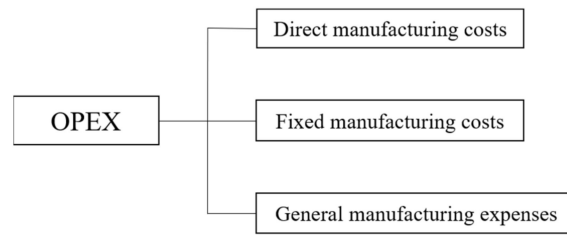


Figure 3. Composition of OPEX.

Table 2. Cost values for CAPEX and OPEX estimation.

Item	Unit	Value
Operator salary	\$/yr	59,580 [33]
Cooling water cost	\$/MWh	243.68 [33]
Electricity	\$/MWh	26.59 [34]
PEMFC system	\$/kW	100 [35]

The life cycle cost (LCC) is defined as the total costs required to install and operate the system during the life cycle [33]. It is estimated using Equation (7). The specific life cycle cost (SLCC) is defined as the LCC required for 1 kg of BOH, which is estimated using Equation (8). Additionally, the cost difference is defined as the difference between the LH₂ production cost and SLCC, as expressed by Equation (9).

$$LCC = CAPEX + (\text{Life Cycle}) \times OPEX \quad (7)$$

$$SLCC = \frac{LCC}{\dot{m}_{\text{re-liquefaction}}} \quad (8)$$

$$(\text{Cost difference}) = (\text{LH}_2 \text{ production cost}) - SLCC \quad (9)$$

3.3. Restrictions on CO₂ Emissions from LH₂ Carriers

The attained EEDI indicates the CO₂ emissions per unit of deadweight divided by the ship speed, which is calculated using Equation (10) for each ship [36].

$$EEDI_{\text{att}} = \frac{P_{\text{ME}} \cdot C_{\text{ME}} \cdot SFC_{\text{ME}} + P_{\text{AE}} \cdot C_{\text{AE}} \cdot SFC_{\text{AE}}}{DWT \cdot V_{\text{ref}}} \quad (10)$$

P_{ME} : Power of the main engine

P_{AE} : Power of the auxiliary engine

C_{ME} : Conversion factor of the main engine between the fuel consumption and CO₂ emissions

C_{AE} : Conversion factor of the auxiliary engine between the fuel consumption and CO₂ emissions

SFC_{ME} : Specific fuel consumption of the main engine

SFC_{AE} : Specific fuel consumption of the auxiliary engine

DWT: Deadweight of the ship

V_{ref} : Speed of the ship

A diesel electric propulsion obtained using LNG is assumed for LH₂ carriers. Specific fuel consumption is assumed as 175 g/kWh. The conversion factor between the fuel consumption and CO₂ emissions is 2.75 [37]. According to the Marine Environment Protection Committee (MEPC) issued by the IMO, the power of the main engine for diesel electric propulsion is calculated using Equation (11). The parameter η is taken as 91.3 %, which indicates the product of the electrical efficiencies of the generators, transformers,

converters and motors. Considering ships whose rated output of the motor is larger than 10,000 kW, the power of the auxiliary engine is calculated using Equation (12) [36].

$$P_{ME} = 0.83 \times \frac{MPP_{motor}}{\eta} \quad (11)$$

$$P_{AE} = 0.025 \times MPP_{motor} + 250 \text{ kW} \quad (12)$$

MPP_{motor} : Rated output of the motor

η : Product of the electrical efficiencies of the generator, transformer, converter, and motor

The PEMFC system uses the BOH to generate electricity, which is then utilized for propulsion in conjunction with the electricity from the main engine. Therefore, the required power of the main engine is calculated using Equation (13). In this study, the efficiency of the PEMFC system is assumed to be 42% compared with lower heating value of hydrogen. In the case of LNG carriers with a BOG re-liquefaction system, the power required for the BOG re-liquefaction is added to the auxiliary engine power, as shown in Equation (14).

$$P_{ME} = 0.83 \times \frac{MPP_{motor}}{\eta} - P_{PEMFC} \quad (13)$$

$$P_{AE} = 0.025 \times MPP_{motor} + 250 \text{ kW} + P_{re-liq} \quad (14)$$

P_{PEMFC} : Electricity generated from the PEMFC

P_{re-liq} : Power required for re-liquefaction

The required EEDI indicates the criteria that the ship under EEDI regulations must satisfy. Equations (15)–(17) show the methodology for calculating the required EEDI [36].

$$EEDI_{ref} = a \cdot b^{-c} \quad (15)$$

$$EEDI_{req} = (1 - X) \times EEDI_{ref} \quad (16)$$

$$EEDI_{att} \leq EEDI_{req} \quad (17)$$

$EEDI_{ref}$: Reference EEDI

$EEDI_{req}$: Required EEDI

The parameters a and c in the required EEDI equation are determined based on the type of ships. The variable b is the deadweight of the ship. X , which is between 0 and 1, is a reduction factor that indicates the reinforcement of the regulations over time. The time factor (referred to as the 'phase') represents the reinforcement of the regulations over time, which is determined using the value of X . For example, phase 3 indicates the year after 2025 and the factor X in this time is 0.3.

Because the EEDI regulations for LH₂ carriers have not yet been designated, various perspectives should be considered before determining the final designation. This study considers the following EEDI candidates:

- EEDI Candidate 1: EEDI equivalent to that of LNG carriers
- EEDI Candidate 2: EEDI considering the energy density of LH₂
- EEDI Candidate 3: No restrictions using LNG as a fuel

3.4. EEDI Candidate 1: EEDI Equivalent to That of LNG Carriers

The concept behind EEDI candidate 1 is to utilize the required EEDI of LNG carriers for LH₂ carriers. Table 3 shows the parameters used for the evaluation of the required EEDI of LNG carriers. In this EEDI candidate, the parameters in Table 3 and the deadweight of the LH₂ carrier are used to calculate the required EEDI for LH₂ carriers. Therefore, the required EEDI of an LNG carrier with the same deadweight as the LH₂ carrier is calculated and compared with the attained EEDI for the LH₂ carrier.

Table 3. Parameters and variables for the required EEDI of LNG carriers.

Ship Type	<i>a</i>	<i>b</i>	<i>c</i>	<i>X</i>
LNG carrier	2253.70	Deadweight (tons)	0.474	0.3 (Phase 3)

3.5. EEDI Candidate 2: EEDI Considering the Energy Density of LH₂

EEDI candidate 2 considers the energy density difference between LH₂ and LNG. As shown in Table 4, the density of LH₂ is 16% of that of LNG. This low density of LH₂ makes the attained EEDI of an LH₂ carrier calculated using Equation (10) smaller than that of an LNG carrier with the same volumetric capacity. Conversely, LH₂ has a heating value that is 2.58 times that of LNG. This indicates that LH₂ can carry more energy within the same mass as LNG. EEDI candidate 2, therefore, considers this energy density factor. The energy density is used to introduce the “re-scaled deadweight” concept shown in Equation (19) in place of the mass density. Using this rescaled deadweight, Equation (20) defines the “energy-based EEDI”, which applies the energy density concept to the attained EEDI. In EEDI candidate 2, it is compared with the required EEDI of LNG carriers with the same volumetric capacity.

$$DWT = DWT_{\text{cargo}} + DWT_{\text{other}} \quad (18)$$

$$DWT_{\text{re-scaled}} = \frac{LHV_{\text{LH}_2}}{LHV_{\text{LNG}}} DWT_{\text{cargo}} + DWT_{\text{other}} \quad (19)$$

$$EEDI_{\text{energy-based}} = \frac{P_{\text{ME}} \cdot C_{\text{ME}} \cdot \text{SFC}_{\text{ME}} + P_{\text{AE}} \cdot C_{\text{AE}} \cdot \text{SFC}_{\text{AE}}}{DWT_{\text{re-scaled}} \cdot V_{\text{ref}}} \quad (20)$$

DWT_{cargo} : Deadweight of cargo

DWT_{other} : Deadweight without cargo

$DWT_{\text{re-scaled}}$: Rescaled deadweight

LHV_{LH_2} : Lower heating value of LH₂

LHV_{LNG} : Lower heating value of LNG

$EEDI_{\text{energy-based}}$: Energy-based EEDI

Table 4. Densities and lower heating values of LH₂ and LNG.

Item	Units	LNG	LH ₂	Ratio of LH ₂ /LNG
Density	kg/m ³	437.89	70.83	0.16
Gravimetric lower heating value	MWh/kg	12.92	33.33	2.58
Volumetric lower heating value	MWh/m ³	5660.94	2360.41	0.42

3.6. EEDI Candidate 3: No Restrictions Using LNG as a Fuel

EEDI candidate 3 refers to the case in which LH₂ carriers have no restrictions regarding their CO₂ emissions provided that conventional clean fuels such as LNG are used. Unlike other gas carriers that carry CO₂-rich fuels, such as LPG and LNG, LH₂ carriers are used to transport CO₂-free hydrogen. The strong regulations on CO₂ emissions from LH₂ carriers, such as those considered in EEDI candidates 1 and 2, may thereby be impartial to liquid hydrogen, ultimately preventing the shipping of this clean fuel. It would therefore be fair to impose no restrictions on CO₂ emissions if these ships utilize relatively clean fuels such as LPG or LNG. In this case, the practicality of BOH re-liquefaction can be determined purely on an economic basis.

4. Case Study

4.1. Target Ship Descriptions

LH₂ carriers with five different sizes are considered for the subsequent case studies. The data of LNG carriers from the Clarksons database is used to assume the cargo capacity,

rated output of motors for propulsion, and deadweight of LH₂ carriers [38]. The deadweight of an LH₂ carrier is assumed to be sum of the LH₂ cargo weight and the deadweight of an LNG carrier without cargo and with the same capacity. The rated output of the motor (MPP) is calculated to have the same propulsion power of an LNG carrier with the same capacity. Table 5 shows the specifications of the LH₂ carriers based on these assumptions.

Table 5. Specifications of the ship assumptions.

Ship	Cargo Capacity (m ³)	Speed (knots)	MPP (MW)	Dead Weight (tons)
Ship #1	50,000	19	11.49	6300
Ship #2	74,000	17.5	14.02	9400
Ship #3	154,000	19	23.40	19,800
Ship #4	174,000	19	26.00	23,000
Ship #5	210,000	19.5	27.68	24,400

4.2. Voyage Conditions

The LH₂ export terminal is assumed to be located at Darwin, Australia, while the import terminal is assumed to be located at Pyeongtaek, South Korea. The boil-off rate for a laden voyage is assumed to be 0.2%/day [29]. The BOH generation for a ballast voyage is assumed to be 40% of that of the laden voyage. Table 6 shows the voyage conditions between Darwin and Pyeongtaek. Table 7 shows the BOH generation rates for the laden and ballast voyages. Table 8 shows the total amounts of BOH generated during one-way trips.

Table 6. Summary of the voyage conditions from Darwin to Pyeongtaek.

Item	Unit	Value
Distance	km	5600
Voyage time	days	7
Loading time	days	2
Unloading time	days	2
BOR	%/day	0.2

Table 7. BOH generation during voyage.

Voyage	Ship	Unit	Value
Laden voyage	Ship #1	kg/day	6400
	Ship #2	kg/day	9500
	Ship #3	kg/day	19,900
	Ship #4	kg/day	22,400
	Ship #5	kg/day	27,000
Ballast voyage	Ship #1	kg/day	2600
	Ship #2	kg/day	3800
	Ship #3	kg/day	7900
	Ship #4	kg/day	9000
	Ship #5	kg/day	10,800

Table 8. Total amount of BOH during voyage.

Voyage	Case	Unit	Value
Laden voyage	Ship #1	Tons	58
	Ship #2	Tons	86
	Ship #3	Tons	179
	Ship #4	Tons	201
	Ship #5	Tons	243
Ballast voyage	Ship #1	Tons	23
	Ship #2	Tons	34
	Ship #3	Tons	72
	Ship #4	Tons	81
	Ship #5	Tons	97

4.3. Liquid Hydrogen Production Cost

An LH₂ production cost is assumed for comparison with the LCC of the BOH re-liquefaction system. The Fuel Cells Program Records from the Department of Energy provides the costs for hydrogen production and liquefaction. These documents also provide the terminal cost of LH₂ [39,40]. As a result, the total cost for LH₂ production and shipping is assumed to be 6.5 \$/kg as described in Table 9.

Table 9. LH₂ production cost assumption.

Item	Unit	Value
LH ₂ production cost	\$/kg	6.50

5. Results and Discussion

5.1. Energy and Exergy Efficiency Results

Figure 4 shows the SEC of the proposed BOH re-liquefaction system, which varies from 8.22 to 10.80 kWh/kg as the R/G fraction varies from 10% to 100%. The BOH that is diverted to the PEMFC cools down the helium refrigerant through HX 1 and HX 3. As the temperature of the helium at the inlet of the compressors decreases, the specific volume of the helium also decreases. The compressor work required to achieve a specific pressure ratio decreases as this specific volume decreases. In the 100% re-liquefaction case, the temperature of the helium increases from 311 to 486 K during compression from 1.20 to 2.89 bar in Comp 1. In this case, a specific compressor work of 907.94 kJ/kg is required. Conversely, in the 10% re-liquefaction case, the cold BOH heading to the PEMFC stacks cools down the helium refrigerant in HX 3. The inlet temperature of Comp 1 is 240 K and increases to 375 K during compression from 1.20 to 2.89 bar in Comp 1. In this case, the specific compressor work is 700.91 kJ/kg. By comparing the 100% to the 10% R/G fraction, the cold energy from BOH reduces 23% of the required compressor work. As noted for the compression at Comp 1, the cold energy from the BOH reduces the compressor work of Comp 2. In the 100% re-liquefaction case, the inlet and outlet temperatures are 313 and 582 K at Comp 2, respectively, where the helium refrigerant is compressed from 2.89 to 10 bar via 1396.85 kJ/kg of specific compressor work. Similarly, the BOH cools down the helium in the 10% re-liquefaction case. The inlet and outlet temperatures are 240 and 446 K, respectively, with same pressure ratio in the 10% re-liquefaction case, and the specific compressor work is 1071.37 kJ/kg. By comparing the effects of 100% and 10% R/G fractions at Comp 2, the cold energy from the BOH reduces 23% of the required compressor work.

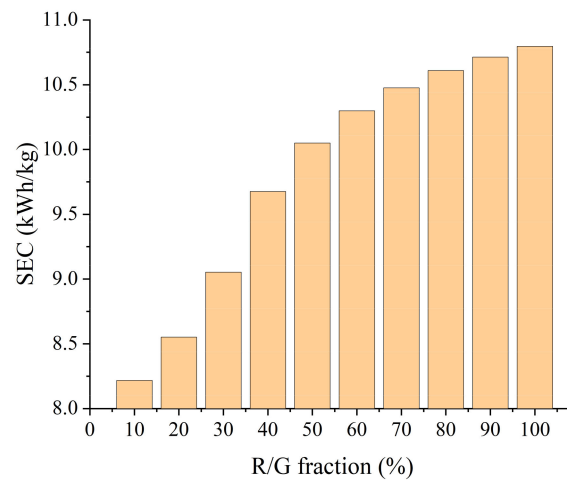


Figure 4. SEC with varying R/G fraction.

Figure 5 shows the exergy efficiency of the BOH re-liquefaction system with varied R/G fractions. The exergy efficiency increases from 0.209 to 0.258 as the R/G fraction increases from 10% to 30%, and it then converges after an R/G fraction of 30%. Figure 6 shows the exergy loss at each component in the re-liquefaction system. The exergy loss in the expanders and compressors is caused by mechanical irreversibility. The exergy loss in the after-coolers and heat exchangers is caused by the heat transfer between a finite temperature difference. It should be mentioned that the exergy loss due to heat transfer decreases as the R/G fraction increases from 10% to 30%, while it converges after 30%. When the R/G fraction is lower than 30%, the excess cold energy is provided by the BOH heading to the PEMFC. The excess cold energy enlarges the temperature difference between the helium and BOH heading to the PEMFC, and this large temperature difference causes a large amount of exergy loss.

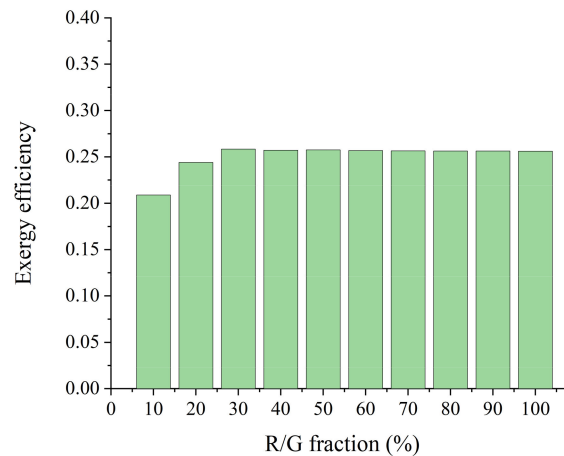


Figure 5. Exergy efficiency with varied R/G fractions.

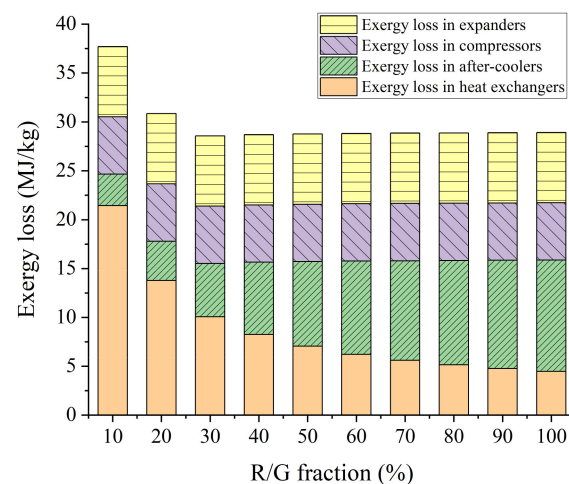


Figure 6. Specific exergy loss with varied R/G fractions.

In the process flow diagram depicted in Figure 1, Stream 108 indicates the BOH diverted to the PEMFC stacks. This stream provided cold energy through HX 3 and HX 1 and is designed to be 310 K, which is the ambient temperature. However, in the cases of 10% and 20% re-liquefaction, the excess cold energy is not fully utilized, and the temperature of Stream 108 is lower than 310 K. Because of this low temperature of Stream 108, the temperature differences in HX 1 and HX 2 are larger than those in the higher R/G fraction cases. As a result, increased exergy losses of 58% and 15% are generated by the heat transfer at the 10% and 20% R/G fractions, respectively, compared to the other R/G fraction cases.

5.2. Economic Evaluation Results

Figure 7 shows the structures of the LCCs for the BOH re-liquefaction systems. It is indicated that OPEX, which includes the operation and maintenance expenses, more influences the LCC than CAPEX, which contains the initial investment of the system. It is obvious that the total LCC increases with the increasing LH₂ capacity of the ship. However, the SLCC, which is the LCC per 1 kg of BOH to be re-liquefied, decreases because the increase of the LCC is lower than the increase of the mass of the re-liquefied BOH. Figure 8a shows the SLCC of the BOH re-liquefaction system as it varies with the capacity of the ship and R/G fraction. It is indicated that at the same R/G fraction, the SLCC decreases as the capacity of the ship increases. Moreover, the SLCC decreases as the R/G fraction increases for the same ship. It can be deduced that as the mass of BOH re-liquefaction increases, the SLCC of the BOH re-liquefaction system decreases. Figure 8b shows the SLCC results with the varied mass of the re-liquefied BOH. It is indicated that as the re-liquefied mass increases, the specific LCC decreases. The slope of the graph in Figure 8b decreases as the re-liquefied mass increases. After the re-liquefied mass is greater than 7.2 ton/day, the SLCC converges at 1.5 \$/kg.

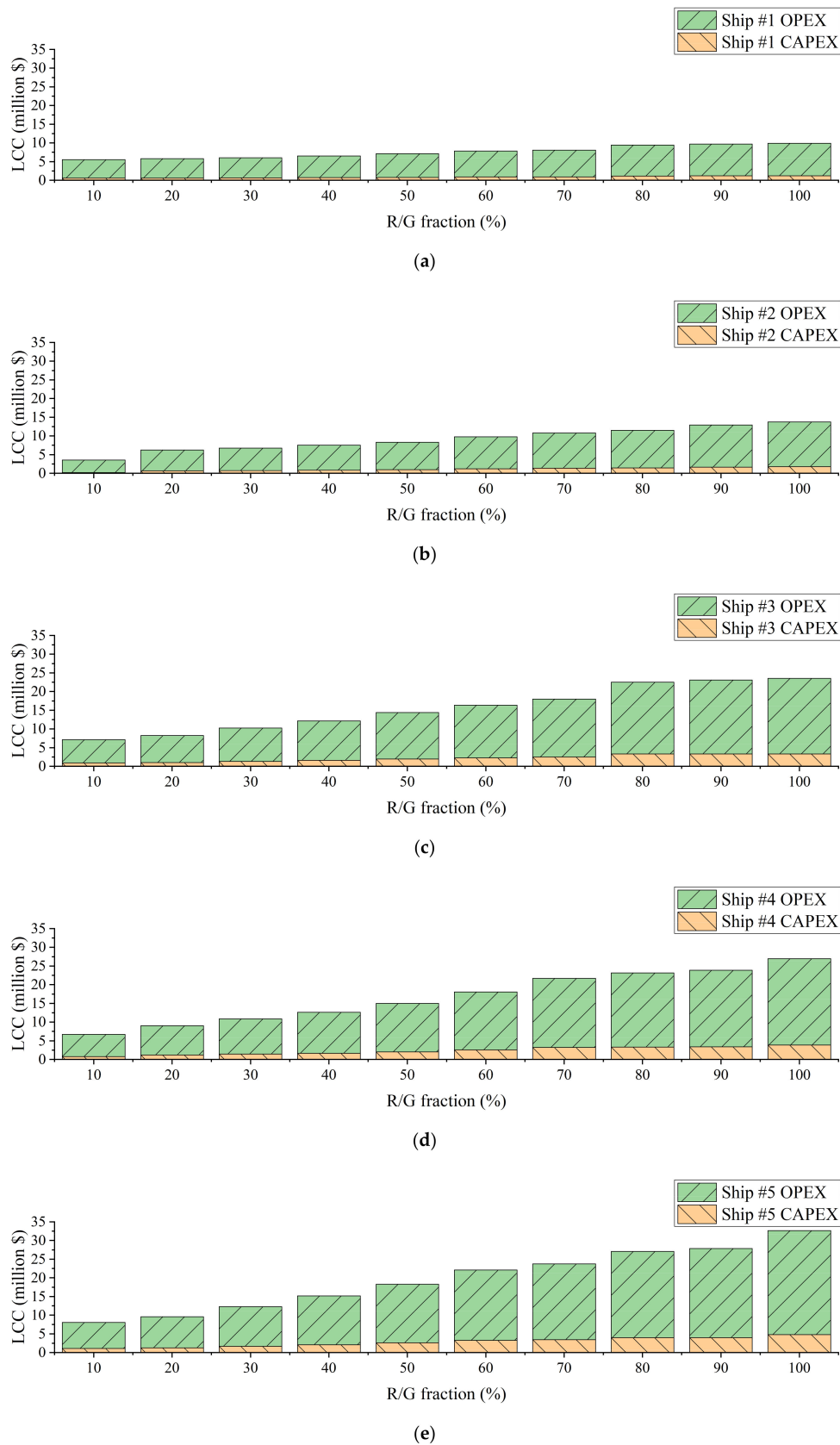


Figure 7. Life cycle cost structures of (a) Ship #1, (b) Ship #2, (c) Ship #3, (d) Ship #4, and (e) Ship #5.

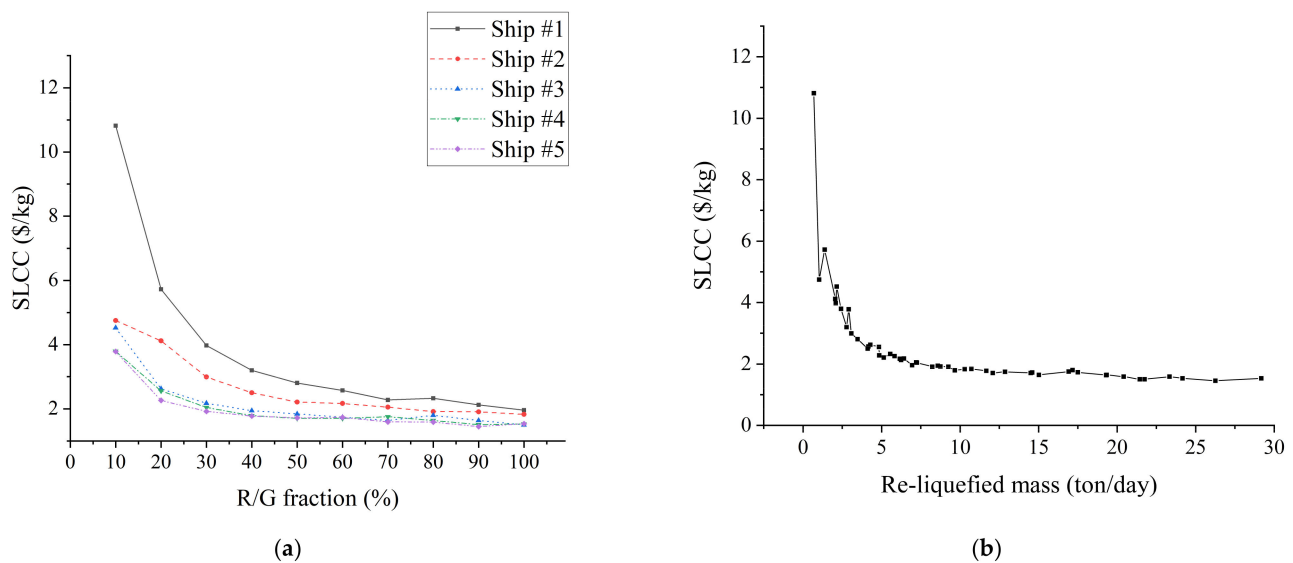


Figure 8. SLCC for each ship with varied (a) R/G fractions and (b) re-liquefied masses.

Compared to the LH_2 production cost of 6.50 \$/kg (as mentioned in Section 4.3), the BOH re-liquefaction system is considered to be beneficial for 20% to 100% R/G fractions. The production cost and SLCC can be used to estimate the economic benefit obtained by using such a system. During the voyage from Darwin to Pyeongtaek described in Section 4.2, the cost difference between the LH_2 production cost and SLCC for a round-trip is estimated in Figure 9.

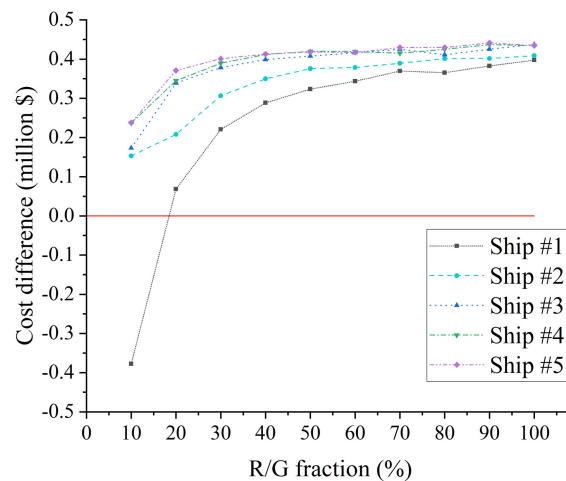


Figure 9. Cost difference with varied R/G fractions during the voyage.

5.3. Consequences of the EEDI

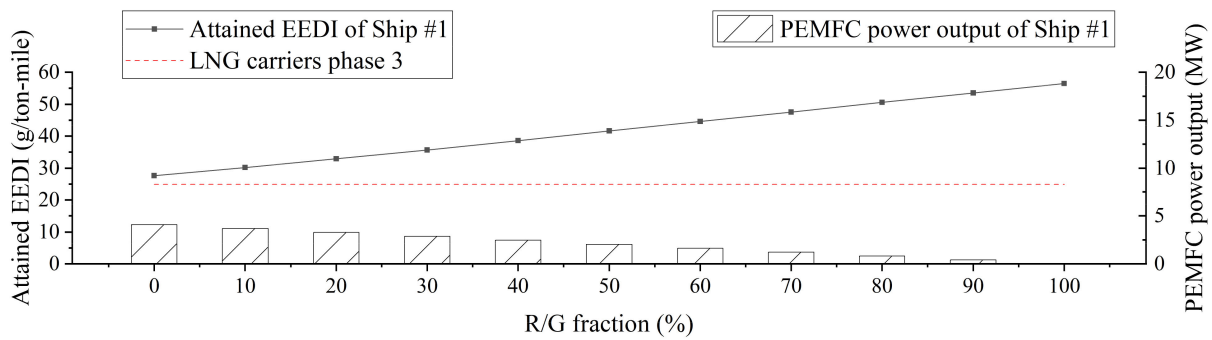
5.3.1. EEDI Candidate 1

Figure 10 shows the attained EEDI results of the ships with varied R/G fractions. Each graph includes the required EEDI phase 3 line of the LNG carrier with the same volumetric capacity. As shown in Equation (10), the calculation results obtained using the same R/G fraction for each ship tend to decrease as the volume capacity of the ships increase. This indicates that as the volumetric capacity of the ship increases, the attained EEDI of the LH_2 carriers tends to decrease and becomes more similar to EEDI candidate 1. As the R/G fraction increases, the BOH utilized in the PEMFC decreases and the required power from the main engine increases. The more power the main engine generates using the LNG fuel, the more CO_2 the ship emits.

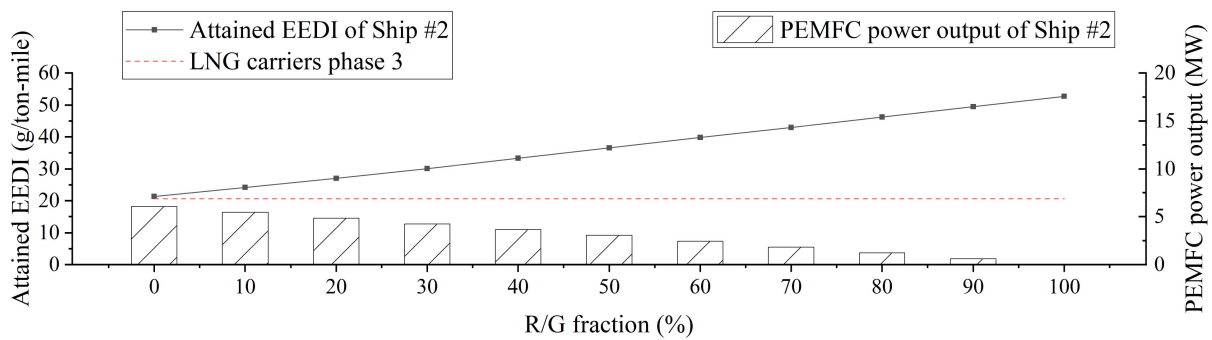
Table 10 shows the permissible R/G fractions according to EEDI candidate 1, indicating that only a small amount of BOH is permissible for re-liquefaction. In the cases of Ships #1 and #2, whose capacity is relatively smaller than the other LH₂ carriers, additional hydrogen is required to satisfy the EEDI candidate 1. Additionally, in the cases of Ships #3 to #5 with larger capacities, less than 15% of the generated BOH is permissible for re-liquefaction.

Table 10. Permittable R/G fractions of the LH₂ carriers according to EEDI candidate 1.

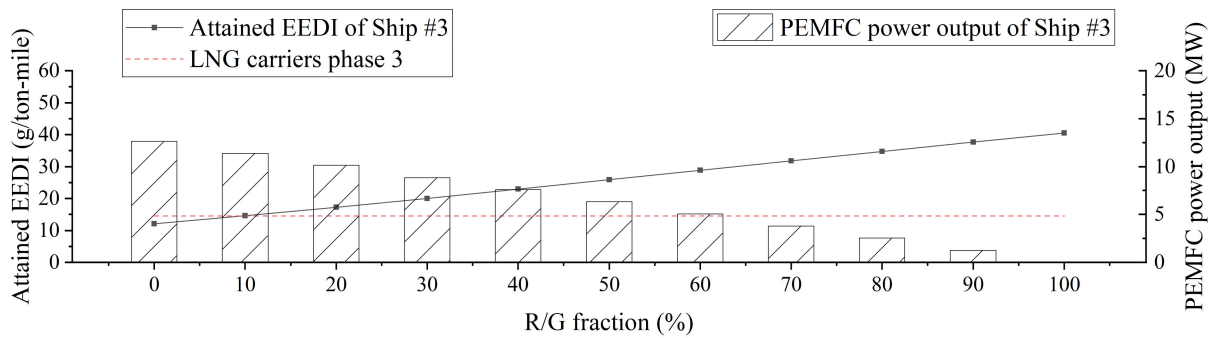
Case	Permittable R/G Fraction (%)
Ship #1	No re-liquefaction
Ship #2	No re-liquefaction
Ship #3	9.37
Ship #4	8.20
Ship #5	14.81



(a)



(b)



(c)

Figure 10. Cont.

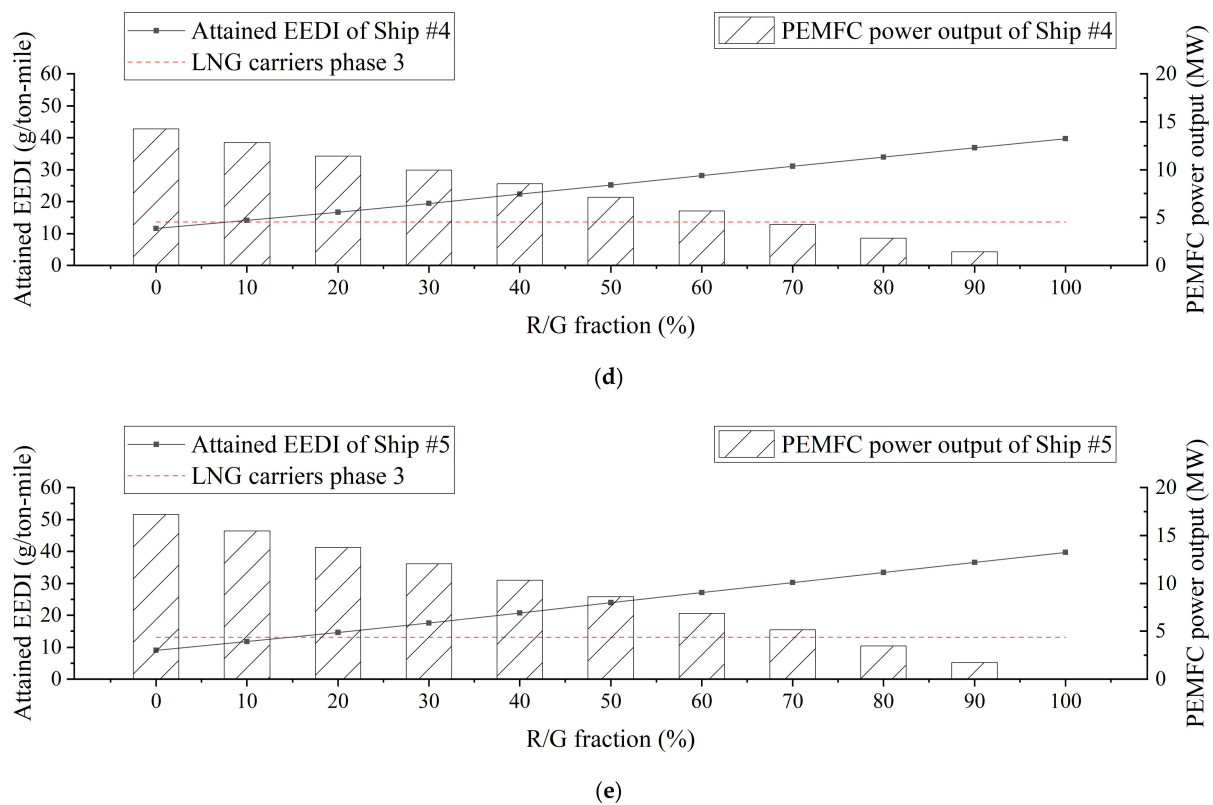


Figure 10. Attained EEDIs for (a) Ship #1, (b) Ship #2, (c) Ship #3, (d) Ship #4, and (e) Ship #5 using EEDI candidate 1.

5.3.2. EEDI Candidate 2

Figure 11 shows the energy-based EEDI calculation results defined for EEDI candidate 2. Each graph for Ships #1 to #5 presents the results of this energy-based EEDI with varied R/G fractions. The graphs also exhibit the required EEDI phase 3 for LNG carriers with the same rescaled deadweight as each LH₂ carrier. Similar to the attained EEDI shown in Figure 10, as the R/G fraction increases, the energy-based EEDI increases. Moreover, the energy-based EEDI tends to decrease as the volumetric capacity of the ships increases. However, unlike the attained EEDI results shown in Figure 10, every ship is able to reliquefy a ratio of BOH between 25% and 33% such that the energy-based EEDI is less than the required EEDI phase 3 of LNG carriers. These results were obtained due to the rescaled deadweight that was increased from the original deadweight considering the differing heating values of LH₂ and LNG. Table 11 shows the permissible R/G fractions of Ships #1 to #5. The permissible R/G fraction tends to increase as the volumetric capacity of the ships increases.

Table 11. Permittable R/G fractions of the LH₂ carriers according to EEDI candidate 2.

Case	Permittable R/G Fraction (%)
Ship #1	26.20
Ship #2	25.45
Ship #3	30.00
Ship #4	27.79
Ship #5	33.35

The differences between Tables 10 and 11 indicate how the mass and energy densities of LH₂ differ from those of LNG. Because LH₂ has a lower density but larger heating value than LNG, the permissible R/G fraction is larger in EEDI candidate 2 than in EEDI candidate 1. The cargo of the currently used energy carriers under EEDI regulations is

mainly hydrocarbon materials such as oil and LNG. These materials have different densities and heating values compared to hydrogen. The existing EEDI regulation for energy carriers, which is calculated using the mass-based deadweight, is used due to the properties of these hydrocarbons. Therefore, the application of this regulation directly to LH₂ carriers without considering the properties of LH₂ is inappropriate. The large heating value of hydrogen should be reflected in these regulations such that the energy carrier may carry energy efficiently.

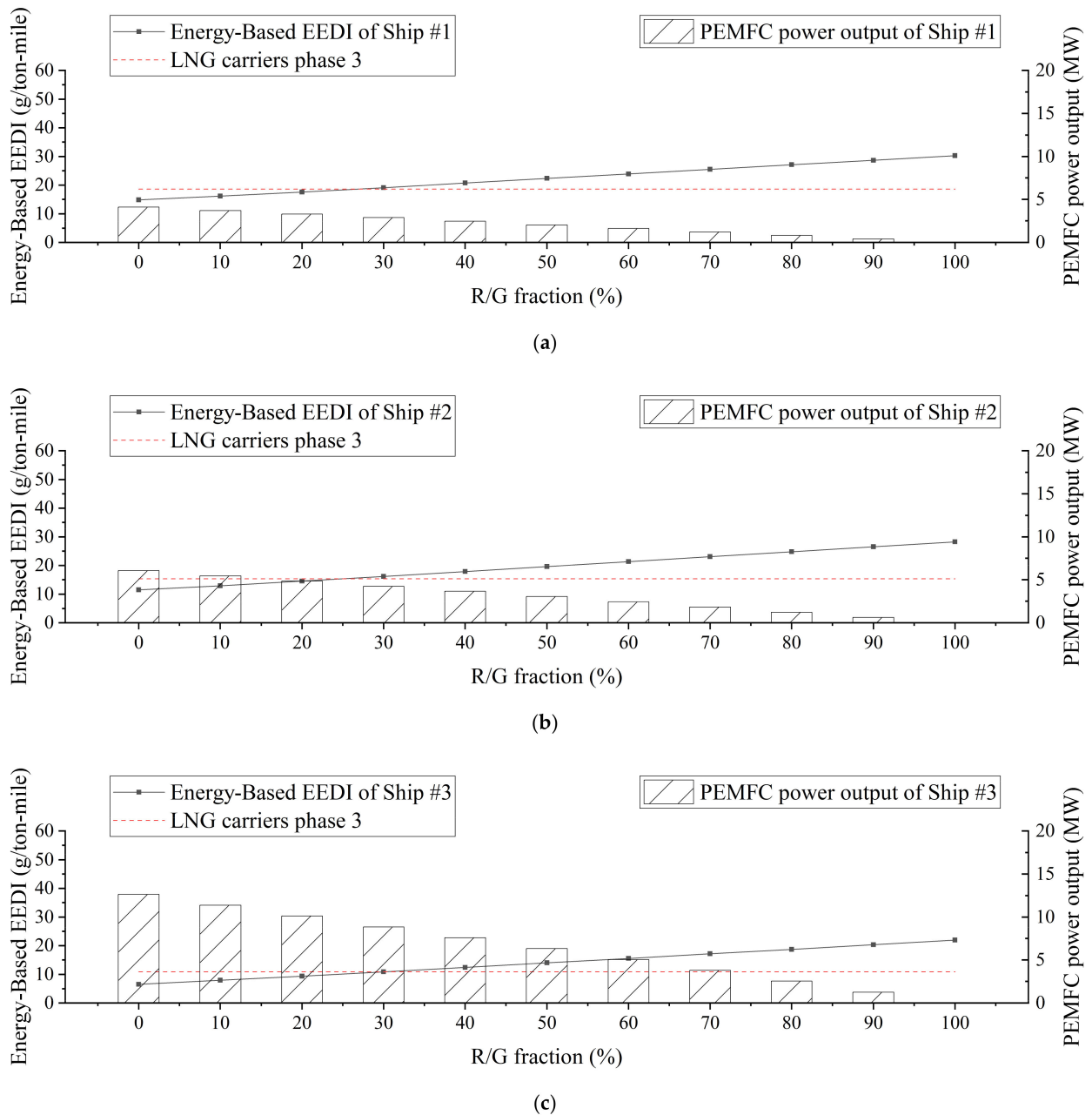


Figure 11. Cont.

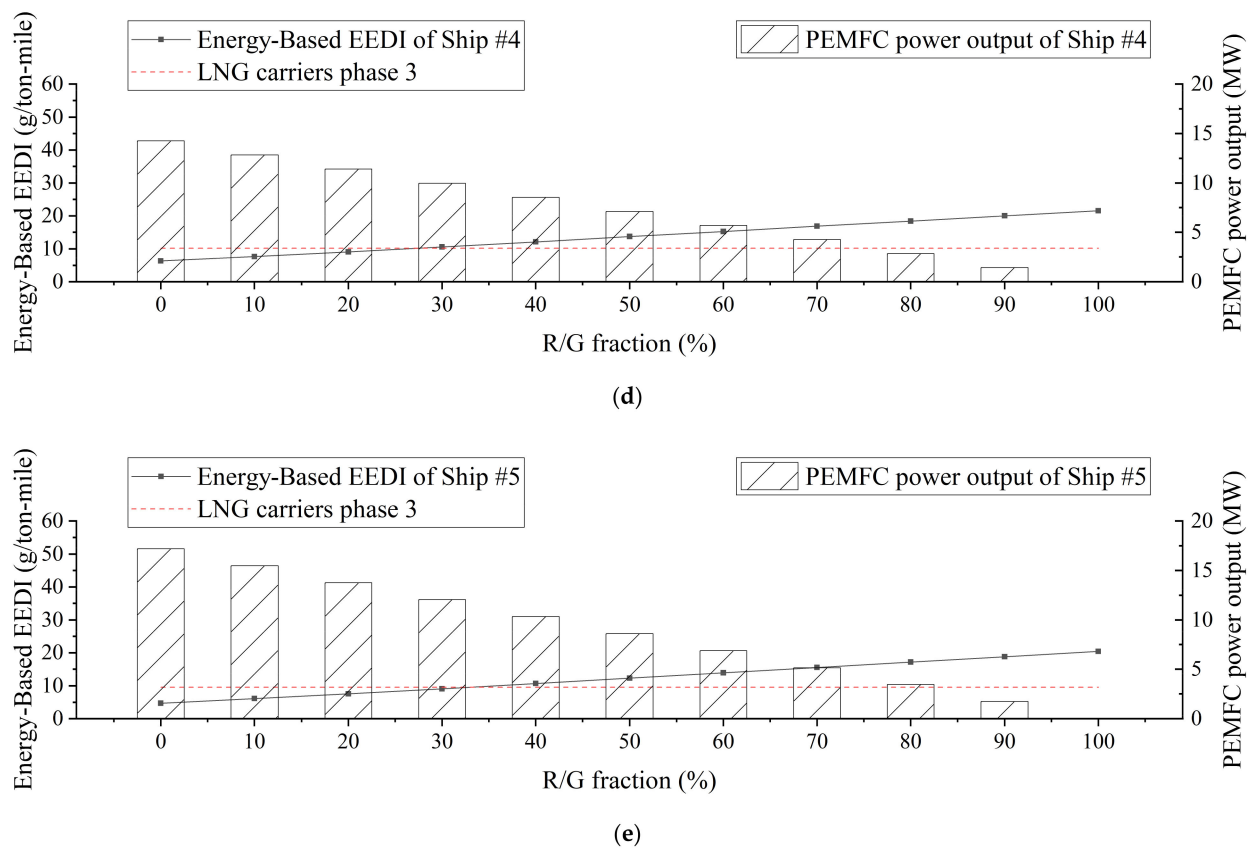


Figure 11. Energy-based EEDIs for (a) Ship #1, (b) Ship #2, (c) Ship #3, (d) Ship #4, and (e) Ship #5 using EEDI candidate 2.

5.3.3. EEDI Candidate 3

EEDI candidate 3 exempts the LH₂ carriers from the EEDI regulations. The LH₂ carriers deliver LH₂ cargo, which emits no CO₂, unlike other fuels. In addition, it is highly likely that only CO₂-free LH₂ will be allowed for international trading. Therefore, although regulations on CO₂ emissions may not be imposed on LH₂ carriers, LH₂ is far less CO₂-intensive than other liquefied cargos such as LNG and LPG considering the entire supply chain.

In this case, the BOH R/G fraction is determined mainly via economic motivations. As discussed in Section 5.2, the SLCC of the BOH re-liquefaction system decreases as the R/G fraction increases. Consequently, all BOH may be re-liquefied considering the economic results obtained using EEDI candidate 3.

Table 12 shows the SLCCs for the permissible R/G fractions obtained using each EEDI candidate. As described in Section 5.3.1, the permissible R/G fraction indicates the amount satisfying the EEDI restrictions for each candidate. In the case of EEDI candidate 3, this ratio is 100% because there is no EEDI restriction. Compared with EEDI candidate 1, the SLCC for the permissible R/G fraction decreases from 50% to 68% depending on the capacity of the LH₂ carriers in EEDI candidate 3. Likewise, the SLCC decreases from 18% to 48% compared to the EEDI candidate 2. These results indicate the economic advantages that may be obtained when LH₂ carriers are not subjected to EEDI restrictions. Considering this advantage and the CO₂-free characteristic of LH₂, the EEDI-free regulation of LH₂ carriers can be considered, which exempts LH₂ carriers with LNG fuels from the CO₂ emissions restrictions.

Table 12. SLCCs for the permissible R/G fractions obtained using each EEDI candidate.

SLCC with EEDI Candidate (\$/kg)	Ship #1	Ship #2	Ship #3	Ship #4	Ship #5
EEDI Candidate 1	-	-	4.64	4.01	3.05
EEDI Candidate 2	4.64	3.51	2.18	2.16	1.87
EEDI Candidate 3	1.96	1.83	1.50	1.53	1.53

6. Conclusions

This study proposed a partial BOH re-liquefaction system based on the reverse Brayton helium cycles. This system divides the generated BOH into two streams, one of which is to be re-liquefied and the other is utilized to generate electricity in PEMFC stacks. Various evaluations for the system were performed based on an assumed voyage route, five different LH₂ carrier specifications, and an assumed LH₂ production cost.

The SEC increased from 8.22 to 10.80 kWh/kg as the R/G fraction increased from 10% to 100%. The exergy efficiency was increased from 0.209 to 0.258 as the R/G fraction increased from 10% to 30%, and it converged to 0.258 when the R/G fraction was larger than 30%. The exergy loss in heat transfer occupied the largest portion of all. Due to the excessive cold energy of the BOH heading to the PEMFC stacks, compared to other R/G fraction cases, 58% and 15% more exergy loss occurred in 10% and 20% cases, respectively.

The system economics indicated that the re-liquefied mass of BOH is inversely proportional to the SLCC. The gradient of this decrease became smoother as the re-liquefied mass of BOH increased. When the re-liquefied mass of BOH was larger than 7200 kg/day, the SLCC was almost unchanged from 1.5 \$/kg; this value is much lower than 6.50 \$/kg, which is the assumed LH₂ production cost.

Considering EEDI candidate 1, the attained EEDI demonstrated that most of the BOH should not be re-liquefied when the required EEDI was evaluated based on the parameters of the LNG carrier for the required EEDI phase 3 with the same volumetric capacity. However, for EEDI candidate 2, it was shown that the permissible R/G fraction was between 25% and 33% considering energy-based EEDI and required EEDI phase 3. Finally, for EEDI candidate 3, the EEDI-free regulation of LH₂ carriers was discussed considering the CO₂-free characteristic of LH₂. If the EEDI regulation is not used for LH₂ carriers, the SLCC of the BOH re-liquefaction system decreases up to 68% compared to LNG carriers with equivalent EEDI regulations.

Author Contributions: Conceptualization, M.C., W.J. and S.L.; methodology, W.J. and T.J.; software, M.C.; validation, M.C. and W.J.; formal analysis, M.C.; investigation, M.C.; resources, T.J.; data curation, M.C.; writing—original draft preparation, M.C.; writing—review and editing, W.J.; visualization, M.C.; supervision, W.J. and D.C.; project administration, D.C.; funding acquisition, D.C. All authors have read and agreed to the published version of the manuscript.

Funding: This research was a part of the project titled ‘Development of Safety and Control Standards for Hydrogen Ships: Cargo Handling and Fuel Gas Supply Systems’ (Grant number: 20200456), funded by the Ministry of Oceans and Fisheries, Korea.

Conflicts of Interest: The authors declare no conflict of interest.

Nomenclature

Scripts	Description
\dot{W}_{net}	Total work required to re-liquefy BOH (kW)
$\dot{W}_{Comp 1}$	Work input for Comp 1 (kW)
$\dot{W}_{Comp 2}$	Work input for Comp 2 (kW)
$\dot{W}_{Exp 1}$	Work output for Exp 1 (kW)
$\dot{W}_{Exp 2}$	Work output for Exp 2 (kW)
$\dot{m}_{BOH-generation}$	Mass flow of the generated BOH (kg/s)

$\dot{m}_{re-liquefaction}$	Mass flow of the re-liquefied BOH (kg/s)
E_S	Physical flow exergy of stream (kJ)
E_T	Thermal exergy of stream (kJ)
E_M	Mechanical exergy of stream (kJ)
H_S	Enthalpy of stream at present state (kJ)
H_{**}	Enthalpy of stream at state ** (kJ)
H_0	Enthalpy of stream at dead state (kJ)
S_S	Entropy of stream at present state (kJ/K)
S_{**}	Entropy of stream at state ** (kJ/K)
S_0	Entropy of stream at dead state (kJ/K)
T_0	Ambient temperature (K)
η_{ex}	Exergy efficiency
$\dot{E}_{BOH\ to\ PEMFC-in}$	Physical flow exergy of Stream 106 (kW)
$\dot{E}_{BOH\ to\ PEMFC-out}$	Physical flow exergy of Stream 108 (kW)
$\dot{E}_{re-liquefaction-in}$	Physical flow exergy of Stream 102 (kW)
$\dot{E}_{re-liquefaction-out}$	Physical flow exergy of Stream 105 (kW)
C_{OL}	Cost of the operator salary (\$/yr)
C_{UT}	Cost of utilities (\$/GJ)
C_{WT}	Cost of the cooling water (\$/GJ)
$EEDI_{att}$	Attained EEDI (g/ton-mile)
P_{ME}	Power of the main engine (kW)
P_{AE}	Power of the auxiliary engine (kW)
C_{ME}	Conversion factor of the main engine between fuel consumption and CO ₂ emissions
C_{AE}	Conversion factor of the auxiliary engine between fuel consumption and CO ₂ emissions
SFC_{ME}	Specific fuel consumption of the main engine (g/kWh)
SFC_{AE}	Specific fuel consumption of the auxiliary engine (g/kWh)
DWT	Deadweight of the ship (ton)
V_{ref}	Speed of the ship (knot)
MPP_{motor}	Rated output of the motor (kW)
η	Product of the electrical efficiencies of the generator, transformer, converter, and motor
P_{PEMFC}	Electricity generated from the PEMFC (kW)
P_{re-liq}	Power required for re-liquefaction (kW)
$EEDI_{ref}$	Reference EEDI (g/ton-mile)
$EEDI_{req}$	Required EEDI (g/ton-mile)
DWT_{cargo}	Deadweight of cargo (ton)
DWT_{other}	Deadweight without cargo (ton)
$DWT_{re-scaled}$	Re-scaled deadweight (ton)
LHV_{LH2}	Lower heating value of LH ₂ (MJ/kg)
LHV_{LNG}	Lower heating value of LNG (MJ/kg)
$EEDI_{energy-based}$	Energy based EEDI (ton)
Abbreviation	Description
BOG	Boil-off gas
BOH	Boil-off hydrogen
CO ₂	Carbon dioxide
IMO	International Maritime Organization
LCC	Life cycle cost (\$)
LH ₂	Liquid hydrogen
LNG	Liquified natural gas
MEPC	Marine Environment Protection Committee
PEMFC	Proton-exchange membrane fuel cell
R/G fraction	Re-liquefaction-generation fraction (%)
SEC	Specific energy consumption (kWh/kg)
SLCC	Specific life cycle cost (\$/kg)

References

1. NOAA's Annual Greenhouse Gas Index. Available online: <https://www.esrl.noaa.gov/gmd/aggi/> (accessed on 3 May 2021).
2. Total Energy Supply (TES) by Source. Available online: <https://www.iea.org/data-and-statistics/?country=WORLD&fuel=EnergySupply&indicator=TPESbySource> (accessed on 3 May 2021).
3. Total CO₂ Emissions. Available online: <https://www.iea.org/data-and-statistics/?country=WORLD&fuel=CO2emissions&indicator=TotCO2> (accessed on 3 May 2021).
4. Renewable Electricity Generation by Source (Non-Combustible). Available online: <https://www.iea.org/data-and-statistics/?country=WORLD&fuel=EnergySupply&indicator=RenewGenBySource> (accessed on 3 May 2021).
5. Share of Renewables in Power Generation in the Sustainable Development Scenario, 2000–2030. Available online: <https://www.iea.org/data-and-statistics/charts/share-of-renewables-in-power-generation-in-the-sustainable-development-scenario-2000-2030> (accessed on 6 May 2021).
6. Pethaiah, S.S.; Sadasivuni, K.K.; Jayakumar, A.; Ponnamma, D.; Tiwary, C.S.; Sasikumar, G. Methanol Electrolysis for Hydrogen Production Using Polymer Electrolyte Membrane: A Mini-Review. *Energies* **2020**, *13*, 5879. [\[CrossRef\]](#)
7. Jayakumar, A. *An Assessment on Polymer Electrolyte Membrane (PEM) Fuel Cell Stack Components*; Apple Academic Press: Boca Raton, FL, USA, 2017; ISBN 9781771886062.
8. Rosen, M.A.; Koochi-Fayegh, S. The prospects for hydrogen as an energy carrier: An overview of hydrogen energy and hydrogen energy systems. *Energy Ecol. Environ.* **2016**, *1*, 10–29. [\[CrossRef\]](#)
9. Niaz, S.; Manzoor, T.; Pandith, A.H. Hydrogen storage: Materials, methods and perspectives. *Renew. Sustain. Energy Rev.* **2015**, *50*, 457–469. [\[CrossRef\]](#)
10. Yanxing, Z.; Maoqiong, G.; Yuan, Z.; Xueqiang, D.; Jun, S. Thermodynamics analysis of hydrogen storage based on compressed gaseous hydrogen, liquid hydrogen and cryo-compressed hydrogen. *Int. J. Hydrog. Energy* **2019**, *44*, 16833–16840. [\[CrossRef\]](#)
11. Notardonato, W.U.; Swanger, A.M.; Fesmire, J.E.; Jumper, K.M.; Johnson, W.L.; Tomsik, T.M. Zero boil-off methods for large-scale liquid hydrogen tanks using integrated refrigeration and storage. *IOP Conf. Ser. Mater. Sci. Eng.* **2017**, *278*, 012012. [\[CrossRef\]](#)
12. Tan, H.; Zhao, Q.; Sun, N.; Li, Y. Enhancement of energy performance in a boil-off gas re-liquefaction system of LNG carriers using ejectors. *Energy Convers. Manag.* **2016**, *126*, 875–888. [\[CrossRef\]](#)
13. Choi, J. Development of partial liquefaction system for liquefied natural gas carrier application using exergy analysis. *Int. J. Nav. Archit. Ocean Eng.* **2018**, *10*, 609–616. [\[CrossRef\]](#)
14. Sayyaadi, H.; Babaelahi, M. Multi-objective optimization of a joule cycle for re-liquefaction of the Liquefied Natural Gas. *Appl. Energy* **2011**, *88*, 3012–3021. [\[CrossRef\]](#)
15. Kim, D.; Hwang, C.; Gundersen, T.; Lim, Y. Process design and economic optimization of boil-off-gas re-liquefaction systems for LNG carriers. *Energy* **2019**, *173*, 1119–1129. [\[CrossRef\]](#)
16. Romero, J.; Orosa, J.A.; Oliveira, A.C. Research on the Brayton cycle design conditions for reliquefaction cooling of LNG boil off. *J. Mar. Sci. Technol.* **2012**, *17*, 532–541. [\[CrossRef\]](#)
17. Kwak, D.H.; Heo, J.H.; Park, S.H.; Seo, S.J.; Kim, J.K. Energy-efficient design and optimization of boil-off gas (BOG) re-liquefaction process for liquefied natural gas (LNG)-fuelled ship. *Energy* **2018**, *148*, 915–929. [\[CrossRef\]](#)
18. Yin, L.; Ju, Y.L. Comparison and analysis of two nitrogen expansion cycles for BOG Re-liquefaction systems for small LNG ships. *Energy* **2019**, *172*, 769–776. [\[CrossRef\]](#)
19. Sayyaadi, H.; Babaelahi, M. Thermo-economic optimization of a cryogenic refrigeration cycle for re-liquefaction of the LNG boil-off gas. *Int. J. Refrig.* **2010**, *33*, 1197–1207. [\[CrossRef\]](#)
20. Krasae-in, S.; Stang, J.H.; Neksa, P. Development of large-scale hydrogen liquefaction processes from 1898 to 2009. *Int. J. Hydrogen Energy* **2010**, *35*, 4524–4533. [\[CrossRef\]](#)
21. Krasae-In, S.; Stang, J.H.; Neksa, P. Exergy analysis on the simulation of a small-scale hydrogen liquefaction test rig with a multi-component refrigerant refrigeration system. *Int. J. Hydrog. Energy* **2010**, *35*, 8030–8042. [\[CrossRef\]](#)
22. Ratlamwala, T.A.H.; Dincer, I.; Gadalla, M.A. Thermodynamic analysis of a novel integrated geothermal based power generation-quadruple effect absorption cooling-hydrogen liquefaction system. *Int. J. Hydrog. Energy* **2012**, *37*, 5840–5849. [\[CrossRef\]](#)
23. Chang, H.M.; Ryu, K.N.; Baik, J.H. Thermodynamic design of hydrogen liquefaction systems with helium or neon Brayton refrigerator. *Cryogenics* **2018**, *91*, 68–76. [\[CrossRef\]](#)
24. Asadnia, M.; Mehrpooya, M. A novel hydrogen liquefaction process configuration with combined mixed refrigerant systems. *Int. J. Hydrog. Energy* **2017**, *42*, 15564–15585. [\[CrossRef\]](#)
25. Sadaghiani, M.S.; Mehrpooya, M. Introducing and energy analysis of a novel cryogenic hydrogen liquefaction process configuration. *Int. J. Hydrog. Energy* **2017**, *42*, 6033–6050. [\[CrossRef\]](#)
26. Chang, H.M.; Kim, B.H.; Choi, B. Hydrogen liquefaction process with Brayton refrigeration cycle to utilize the cold energy of LNG. *Cryogenics* **2020**, *108*, 103093. [\[CrossRef\]](#)
27. Yuksel, Y.E.; Ozturk, M.; Dincer, I. Analysis and assessment of a novel hydrogen liquefaction process. *Int. J. Hydrog. Energy* **2017**, *42*, 11429–11438. [\[CrossRef\]](#)
28. Lee, H.; Shao, Y.; Lee, S.; Roh, G.; Chun, K.; Kang, H. Analysis and assessment of partial re-liquefaction system for liquefied hydrogen tankers using liquefied natural gas (LNG) and H₂ hybrid propulsion. *Int. J. Hydrog. Energy* **2019**, *44*, 15056–15071. [\[CrossRef\]](#)

29. Ishimoto, Y.; Voldsund, M.; Neksa, P.; Roussanaly, S.; Berstad, D.; Gardarsdottir, S.O. Large-scale production and transport of hydrogen from Norway to Europe and Japan: Value chain analysis and comparison of liquid hydrogen and ammonia as energy carriers. *Int. J. Hydrog. Energy* **2020**, *45*, 32865–32883. [CrossRef]
30. Bejan, A. *Advanced Engineering Thermodynamics*, 3rd ed.; John Wiley & Sons: Hoboken, NJ, USA, 2006; ISBN 9781119245964.
31. Morosuk, T.; Tsatsaronis, G. Splitting physical exergy: Theory and application. *Energy* **2019**, *167*, 698–707. [CrossRef]
32. Tsatsaronis, G.; Morosuk, T. Advanced exergetic analysis of a novel system for generating electricity and vaporizing liquefied natural gas. *Energy* **2010**, *35*, 820–829. [CrossRef]
33. Turton, R.; Bailie, R.C.; Whiting, W.B.; Shaeiwitz, J.A. *Analysis, Synthesis and Design of Chemical Processes*, 4th ed.; Prentice Hall: Upper Saddle River, NJ, USA, 2012.
34. Federal Energy Regulatory Commission Market Assessments. Available online: <https://cms.ferc.gov/sites/default/files/2020-11/ngas-ovr-archive.pdf> (accessed on 10 May 2021).
35. Moreno, N.G.; Molina, M.C.; Gervasio, D.; Robles, J.F.P. Approaches to polymer electrolyte membrane fuel cells (PEMFCs) and their cost. *Renew. Sustain. Energy Rev.* **2015**, *52*, 897–906. [CrossRef]
36. 2018 Guidelines on The Method of Calculation of The Attained Energy Efficiency Design Index (Eedi) for New Ships. Available online: [https://wwwcdn.imo.org/localresources/en/KnowledgeCentre/IndexofIMOResolutions/MEPCDocuments/MEPC.308\(73\).pdf](https://wwwcdn.imo.org/localresources/en/KnowledgeCentre/IndexofIMOResolutions/MEPCDocuments/MEPC.308(73).pdf) (accessed on 6 May 2021).
37. Jeong, J.; Seo, S.; You, H.; Chang, D. Comparative analysis of a hybrid propulsion using LNG-LH2 complying with regulations on emissions. *Int. J. Hydrog. Energy* **2018**, *43*, 3809–3821. [CrossRef]
38. Clarksons Research. Available online: <https://www.clarksons.net/portal/> (accessed on 20 July 2021).
39. Connelly, E.; Penev, M.; Elgowainy, A.; Hunter, C. Current Status of Hydrogen Liquefaction Costs. Available online: https://www.hydrogen.energy.gov/pdfs/19001_hydrogen_liquefaction_costs.pdf (accessed on 6 May 2021).
40. Vickers, J.; Peterson, D.; Randolph, K. Cost of Electrolytic Hydrogen Production with Existing Technology. Available online: <https://www.hydrogen.energy.gov/pdfs/20004-cost-electrolytic-hydrogen-production.pdf> (accessed on 6 May 2021).